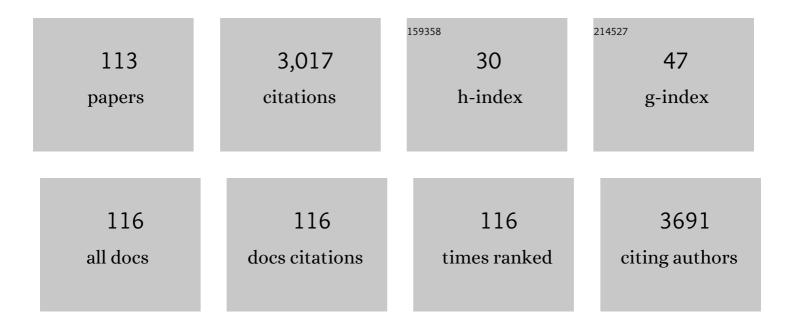
## Marco Merlini

List of Publications by Year in descending order

Source: https://exaly.com/author-pdf/2943754/publications.pdf Version: 2024-02-01



#	Article	IF	CITATIONS
1	Discovery of a Superhard Iron Tetraboride Superconductor. Physical Review Letters, 2013, 111, 157002.	2.9	192
2	Electroactive Ionic Soft Actuators with Monolithically Integrated Gold Nanocomposite Electrodes. Advanced Materials, 2017, 29, 1606109.	11.1	108
3	Structures of dolomite at ultrahigh pressure and their influence on the deep carbon cycle. Proceedings of the National Academy of Sciences of the United States of America, 2012, 109, 13509-13514.	3.3	89
4	Stability of iron-bearing carbonates in the deep Earth's interior. Nature Communications, 2017, 8, 15960.	5.8	84
5	Single-crystal diffraction at megabar conditions by synchrotron radiation. High Pressure Research, 2013, 33, 511-522.	0.4	82
6	Chukanovite, Fe2(CO3)(OH)2, a new mineral from the weathered iron meteorite Dronino. European Journal of Mineralogy, 2007, 19, 891-898.	0.4	79
7	Effect of chemistry on the compressibility of silicate perovskite in the lower mantle. Earth and Planetary Science Letters, 2012, 333-334, 181-190.	1.8	78
8	Single-crystal diffraction at the Extreme Conditions beamline P02.2: procedure for collecting and analyzing high-pressure single-crystal data. Journal of Synchrotron Radiation, 2013, 20, 711-720.	1.0	67
9	Tricalcium aluminate hydration in additivated systems. A crystallographic study by SR-XRPD. Cement and Concrete Research, 2008, 38, 477-486.	4.6	66
10	Phase development in conventional and active belite cement pastes by Rietveld analysis and chemical constraints. Cement and Concrete Research, 2009, 39, 833-842.	4.6	65
11	Single-crystal X-ray diffraction at megabar pressures and temperatures of thousands of degrees. High Pressure Research, 2010, 30, 620-633.	0.4	65
12	Depth of formation of CaSiO 3 -walstromite included in super-deep diamonds. Lithos, 2016, 265, 138-147.	0.6	55
13	High-pressure thermo-elastic properties of beryl (Al4Be6Si12O36) from ab initio calculations, and observations about the source of thermal expansion. Physics and Chemistry of Minerals, 2011, 38, 223-239.	0.3	52
14	The crystal structures of Mg2Fe2C4O13, with tetrahedrally coordinated carbon, and Fe13O19, synthesized at deep mantle conditions. American Mineralogist, 2015, 100, 2001-2004.	0.9	51
15	Portable double-sided laser-heating system for Mössbauer spectroscopy and X-ray diffraction experiments at synchrotron facilities with diamond anvil cells. Review of Scientific Instruments, 2012, 83, 124501.	0.6	50
16	Fe3+ spin transition in CaFe2O4 at high pressure. American Mineralogist, 2010, 95, 200-203.	0.9	44
17	Synthesis of calcium oxalate trihydrate: New data by vibrational spectroscopy and synchrotron X-ray diffraction. Spectrochimica Acta - Part A: Molecular and Biomolecular Spectroscopy, 2015, 150, 721-730.	2.0	44
18	Bottom-up engineering of the surface roughness of nanostructured cubic zirconia to control cell adhesion. Nanotechnology, 2012, 23, 475101.	1.3	43

#	Article	IF	CITATIONS
19	Hydrophobizing coatings for cultural heritage. A detailed study of resin/stone surface interaction. Applied Physics A: Materials Science and Processing, 2014, 116, 341-348.	1.1	43
20	Dolomite-IV: Candidate structure for a carbonate in the Earth's lower mantle. American Mineralogist, 2017, 102, 1763-1766.	0.9	42
21	XAS and GIXRD Study of Co Sites in CoAl <sub>2</sub> O <sub>4</sub> Layers Grown by MOCVD. Chemistry of Materials, 2010, 22, 1933-1942.	3.2	41
22	Magnesium silicate perovskite and effect of iron oxidation state on its bulk sound velocity at the conditions of the lower mantle. Earth and Planetary Science Letters, 2014, 393, 182-186.	1.8	39
23	Thermal expansion and phase transitions in åkermanite and gehlenite. Physics and Chemistry of Minerals, 2005, 32, 189-196.	0.3	35
24	Solvent Induced Pseudopolymorphism in a Calixarene-Based Porous Host Framework. Crystal Growth and Design, 2010, 10, 1527-1533.	1.4	34
25	Growth of Cu2MnSnS4 PV absorbers by sulfurization of evaporated precursors. Journal of Alloys and Compounds, 2017, 693, 95-102.	2.8	34
26	Diammonium hydrogenphosphate for the consolidation of building materials. Investigation of newly-formed calcium phosphates. Construction and Building Materials, 2019, 195, 557-563.	3.2	34
27	High-temperature behaviour of melilite: in situ X-ray diffraction study of gehlenite–åkermanite–Na melilite solid solution. Physics and Chemistry of Minerals, 2008, 35, 147-155.	0.3	32
28	Thermal expansion and stability of Ti2SC in air and inert atmospheres. Journal of Alloys and Compounds, 2009, 469, 395-400.	2.8	32
29	A new hydrous Al-bearing pyroxene as a water carrier in subduction zones. Earth and Planetary Science Letters, 2011, 310, 422-428.	1.8	32
30	On the crystal structure and compressional behavior of talc: a mineral of interest in petrology and material science. Physics and Chemistry of Minerals, 2013, 40, 145-156.	0.3	32
31	Puzzling calcite-III dimorphism: crystallography, high-pressure behavior, and pathway of single-crystal transitions. Physics and Chemistry of Minerals, 2015, 42, 29-43.	0.3	32
32	High temperature stability of Ba0.5Sr0.5Co0.8Fe0.2O3â^' and La0.6Sr0.4Co1Fe O3â^' oxygen separation perovskite membranes. Journal of the European Ceramic Society, 2016, 36, 1679-1690.	2.8	32
33	Effect of high pressure on the crystal structure and electronic properties of magnetite below 25 GPa. American Mineralogist, 2012, 97, 128-133.	0.9	31
34	Single-crystal diffraction at the high-pressure Indo-Italian beamline Xpress at Elettra, Trieste. Journal of Synchrotron Radiation, 2020, 27, 222-229.	1.0	31
35	Evidence of interspersed co-existing CaCO <sub>3</sub> -III and CaCO <sub>3</sub> -IIIb structures in polycrystalline CaCO <sub>3</sub> at high pressure. Mineralogical Magazine, 2014, 78, 225-233.	0.6	30
36	High-pressure compressibility and thermal expansion of aragonite. American Mineralogist, 2016, 101, 1651-1658.	0.9	30

#	Article	IF	CITATIONS
37	Polychrome glass from Etruscan sites: first non-destructive characterization with synchrotron μ-XRF, μ-XANES and XRPD. Applied Physics A: Materials Science and Processing, 2008, 92, 127-135.	1.1	29
38	Pressure-induced isostructural phase transformation in $\hat{I}^3$ -B28. Physical Review B, 2010, 82, .	1.1	27
39	Phase transition at high pressure in Cu <sub>2</sub> CO <sub>3</sub> (OH) <sub>2</sub> related to the reduction of the Jahn–Teller effect. Acta Crystallographica Section B: Structural Science, 2012, 68, 266-274.	1.8	27
40	The high-pressure stability of chlorite and other hydrates in subduction mélanges: experiments in the system Cr2O3–MgO–Al2O3–SiO2–H2O. Contributions To Mineralogy and Petrology, 2014, 167, 1.	1.2	27
41	The early hydration and the set of Portland cements: <i>In situ</i> X-ray powder diffraction studies. Powder Diffraction, 2007, 22, 201-208.	0.4	26
42	High-pressure structural studies of eskolaite by means of single-crystal X-ray diffraction. American Mineralogist, 2012, 97, 1764-1770.	0.9	26
43	Non-ideality and defectivity of the akermanite-gehlenite solid solution: An X-ray diffraction and TEM study. American Mineralogist, 2007, 92, 1685-1694.	0.9	25
44	Thermo-physical properties of as deposited and aged thermal barrier coatings (TBC) for gas turbines: State-of-the art and advanced TBCs. Journal of the European Ceramic Society, 2018, 38, 3945-3961.	2.8	25
45	Cordierite under hydrostatic compression: Anomalous elastic behavior as a precursor for a pressure-induced phase transition. American Mineralogist, 2014, 99, 479-493.	0.9	23
46	Crystal structure, high-pressure, and high-temperature behavior of carbonates in the K <sub>2</sub> Mg(CO <sub>3</sub> ) <sub>2</sub> –Na <sub>2</sub> Mg(CO <sub>3</sub> ) <sub>2</sub> jo American Mineralogist, 2015, 100, 2458-2467.	in.0.9	22
47	AlPO4-5 zeolite at high pressure: Crystal–fluid interaction and elastic behavior. Microporous and Mesoporous Materials, 2016, 228, 158-167.	2.2	22
48	High-temperature and high-pressure behavior of carbonates in the ternary diagram CaCO <sub>3</sub> -MgCO <sub>3</sub> -FeCO <sub>3</sub> . American Mineralogist, 2016, 101, 1423-1430.	0.9	22
49	Highâ€∓emperature Thermal Expansion and Stability of V <sub>2</sub> AlC Up To 950°C. Journal of the American Ceramic Society, 2007, 90, 3013-3016.	1.9	21
50	Long-term leaching test in concretes: An X-ray powder diffraction study. Cement and Concrete Composites, 2008, 30, 700-705.	4.6	21
51	Behavior of epidote at high pressure and high temperature: a powder diffraction study up to 10ÂGPa and 1,200ÂK. Physics and Chemistry of Minerals, 2011, 38, 419-428.	0.3	21
52	Highâ€Pressure Behavior and Phase Stability of <scp><scp>Al</scp></scp> <sub>5</sub> <scp><scp>BO</scp><sub>9</sub>, a Mulliteâ€Type Ceramic Material. Journal of the American Ceramic Society, 2013, 96, 2583-2592.</scp>	1.9	21
53	Crystallization on heating and complex phase behavior of α-cyclodextrin solutions. Journal of Chemical Physics, 2006, 125, 154504.	1.2	20
54	High-pressure behavior of akermanite and gehlenite and phase stability of the normal structure in melilites. American Mineralogist, 2009, 94, 704-709.	0.9	20

#	Article	IF	CITATIONS
55	Compressibility and crystal–fluid interactions in all-silica ferrierite at high pressure. Microporous and Mesoporous Materials, 2015, 218, 42-54.	2.2	20
56	Electron diffraction determination of 11.5 Ã and HySo structures: Candidate water carriers to the Upper Mantle. American Mineralogist, 2016, 101, 2645-2654.	0.9	20
57	Thermal expansion and dehydroxylation of phengite micas. Physics and Chemistry of Minerals, 2008, 35, 367-379.	0.3	19
58	High-pressure structural behavior of Â-Fe2O3 studied by single-crystal X-ray diffraction and synchrotron radiation up to 25 GPa. American Mineralogist, 2011, 96, 1781-1786.	0.9	19
59	Melilite-type and melilite-related compounds: structural variations along the join Sr2â^'x Ba x MgSi2O7 (OÂâ‰ÂxÂâ‰Â2) and high-pressure behavior of the two end-members. Physics and Chemistry of Minerals, 2012, 39, 199-211.	0.3	19
60	High-pressure behavior of synthetic mordenite-Na: an in situ single-crystal synchrotron X-ray diffraction study. Zeitschrift Fur Kristallographie - Crystalline Materials, 2015, 230, 201-211.	0.4	18
61	Efficient artificial mineralization route to decontaminate Arsenic(III) polluted water - the Tooeleite Way. Scientific Reports, 2016, 6, 26031.	1.6	18
62	Electron Diffraction on Flash-Frozen Cowlesite Reveals the Structure of the First Two-Dimensional Natural Zeolite. ACS Central Science, 2020, 6, 1578-1586.	5.3	18
63	The crystal structure of barite, BaSO4, at high pressure. American Mineralogist, 2011, 96, 364-367.	0.9	17
64	The MnCO <sub>3</sub> -II high-pressure polymorph of rhodocrosite. American Mineralogist, 2015, 100, 2625-2629.	0.9	17
65	The bulk modulus of SmFeAs(O0.93F0.07). Physica C: Superconductivity and Its Applications, 2009, 469, 782-784.	0.6	16
66	The temperature and compositional dependence of disordering in Fe-bearing dolomites. American Mineralogist, 2012, 97, 1676-1684.	0.9	16
67	Phase stability and thermo-elastic behavior of CsAlSiO4 (ABW): A potential nuclear waste disposal material. Microporous and Mesoporous Materials, 2012, 163, 147-152.	2.2	16
68	Structural and Electric Evidence of Ferrielectric State in Pb <sub>2</sub> MnWO <sub>6</sub> Double Perovskite System. Inorganic Chemistry, 2014, 53, 10283-10290.	1.9	16
69	Crystal growth in gelled solution: applications to coordination polymers. CrystEngComm, 2016, 18, 2455-2462.	1.3	16
70	Highâ€pressure behavior and <i>P</i> â€induced phase transition of CaB <sub>3</sub> O <sub>4</sub> ( <scp>OH</scp> ) <sub>3</sub> ÂH <sub>2</sub> O (colemanite). Journal of the American Ceramic Society, 2017, 100, 2209-2220.	1.9	16
71	Anisotropic compressional behavior of ettringite. Cement and Concrete Research, 2019, 120, 46-51.	4.6	16
72	On the structure of high-pressure high-temperature ÎO2. Journal of Chemical Physics, 2009, 130, 164516.	1.2	15

#	Article	IF	CITATIONS
73	In situsimultaneous synchrotron powder diffraction and mass spectrometry study of methane anaerobic combustion on iron-oxide-based oxygen carrier. Journal of Applied Crystallography, 2005, 38, 353-360.	1.9	14
74	Inclusion Properties of Volatile Organic Compounds in a Calixarene-Based Organic Zeolite. Langmuir, 2012, 28, 8511-8517.	1.6	14
75	Structural Evolution under Pressure of BiMnO <sub>3</sub> . Inorganic Chemistry, 2014, 53, 8749-8754.	1.9	14
76	High-pressure polymorphism and structural transitions of norsethite, BaMg(CO3)2. Physics and Chemistry of Minerals, 2014, 41, 737-755.	0.3	14
77	Crystal-fluid interactions in laumontite. Microporous and Mesoporous Materials, 2018, 263, 86-95.	2.2	14
78	Temperature dependence of the pressure induced monoclinic distortion in the spin Shastry–Sutherland compound SrCu2(BO3)2. Solid State Communications, 2014, 186, 13-17.	0.9	13
79	The stability and melting of aragonite: An experimental and thermodynamic model for carbonated eclogites in the mantle. Lithos, 2019, 324-325, 105-114.	0.6	13
80	Phase stability of TiH2 under high pressure and temperatures. International Journal of Hydrogen Energy, 2008, 33, 6667-6671.	3.8	12
81	On the crystal chemistry and elastic behavior of a phlogopite 3T. Physics and Chemistry of Minerals, 2011, 38, 655-664.	0.3	12
82	(Na,â–¡) <sub>5</sub> [MnO <sub>2</sub> ] <sub>13</sub> nanorods: a new tunnel structure for electrode materials determined <i>ab initio</i> and refined through a combination of electron and synchrotron diffraction data. Acta Crystallographica Section B: Structural Science, Crystal Engineering and Materials, 2016, 72, 893-903.	0.5	12
83	On the P-induced behavior of the zeolite phillipsite: an in situ single-crystal synchrotron X-ray diffraction study. Physics and Chemistry of Minerals, 2017, 44, 1-20.	0.3	12
84	Synchrotron radiation μ X-ray diffraction in transmission geometry for investigating the penetration depth of conservation treatments on cultural heritage stone materials. Analytical Methods, 2020, 12, 1587-1594.	1.3	12
85	Elastic behaviour and phase stability of pyrophyllite and talc at high pressure and temperature. Physics and Chemistry of Minerals, 2015, 42, 309-318.	0.3	11
86	Structural and magnetic characterization of the double perovskite Pb <sub>2</sub> FeMoO <sub>6</sub> . Journal of Materials Chemistry C, 2016, 4, 1533-1542.	2.7	11
87	Consolidation of building materials with a phosphate-based treatment: Effects on the microstructure and on the 3D pore network. Materials Characterization, 2019, 154, 315-324.	1.9	11
88	Highâ€pressure behavior and phase stability of Na 2 B 4 O 6 (OH) 2 ·3H 2 O (kernite). Journal of the American Ceramic Society, 2020, 103, 5291-5301.	1.9	11
89	Crystal Structure Evolution of CaSiO3 Polymorphs at Earth's Mantle Pressures. Minerals (Basel,) Tj ETQq1 :	1 0.784314 0.8	rgBT /Overloo
90	Thermal behaviour of tobermorite from N'Chwaning II mine (Kalahari Manganese Field, Republic of) Tj ETQq0 0 2012, 24, 981-989.	0 rgBT /Ov 0.4	erlock 10 Tf 5 10

#	Article	IF	CITATIONS
91	What's underneath? A non-destructive depth profile of painted stratigraphies by synchrotron grazing incidence X-ray diffraction. Analyst, The, 2018, 143, 4290-4297.	1.7	10
92	Investigating distribution patterns of airborne magnetic grains trapped in tree barks in Milan, Italy: insights for pollution mitigation strategies. Geophysical Journal International, 2017, 210, 989-1000.	1.0	9
93	Grazing incidence synchrotron X-ray diffraction of marbles consolidated with diammonium hydrogen phosphate treatments: non-destructive probing of buried minerals. Applied Physics A: Materials Science and Processing, 2018, 124, 1.	1.1	9
94	Thermal and compressional behavior of the natural borate kurnakovite, MgB3O3(OH)5·5H2O. Construction and Building Materials, 2021, 266, 121094.	3.2	9
95	Phase transition and high-pressure behavior of ulexite, a potential aggregate in radiation-shielding concretes. Construction and Building Materials, 2021, 291, 123188.	3.2	9
96	The high-pressure monazite-to-scheelite transformation in CaSeO4. Mineralogical Magazine, 2012, 76, 913-923.	0.6	8
97	The high-pressure-high-temperature behavior of bassanite. American Mineralogist, 2009, 94, 1596-1602.	0.9	7
98	High-pressure behavior of davyne [CAN-topology]: An in situ single-crystal synchrotron diffraction study. Microporous and Mesoporous Materials, 2014, 198, 203-214.	2.2	7
99	Highâ€pressure behavior of (Cs,K)Al <sub>4</sub> Be <sub>5</sub> B <sub>11</sub> O <sub>28</sub> (londonite): A singleâ€crystal synchrotron diffraction study up to 26 GPa. Journal of the American Ceramic Society, 2017, 100, 4893-4901.	1.9	7
100	Pargasite at high pressure and temperature. Physics and Chemistry of Minerals, 2018, 45, 259-278.	0.3	7
101	Carbon-Bearing Phases throughout Earth's Interior. , 2019, , 66-88.		7
102	High-pressure behavior of intermediate scapolite: compressibility, structure deformation and phase transition. Physics and Chemistry of Minerals, 2018, 45, 945-962.	0.3	5
103	Armstrongite at non-ambient conditions: An in-situ high-pressure single-crystal X-ray diffraction study. Microporous and Mesoporous Materials, 2019, 274, 171-175.	2.2	5
104	The elastic behavior of zeolitic frameworks: The case of MFI type zeolite under high-pressure methanol intrusion. Catalysis Today, 2020, 345, 88-96.	2.2	5
105	Monazite structure from dehydrated CaSeO <sub>4</sub> ·2H <sub>2</sub> O. Mineralogical Magazine, 2010, 74, 127-139.	0.6	4
106	The thermoelastic behavior of clintonite up to 10ÂGPa and 1,000°C. Physics and Chemistry of Minerals, 2012, 39, 385-397.	0.3	4
107	Covalency-driven structural instability and spin-phonon coupling in barium cobalt oxychloride. Physical Review B, 2014, 90, .	1.1	4
108	Allanite at high pressure: effect of REE on the elastic behaviour of epidote-group minerals. Physics and Chemistry of Minerals, 2019, 46, 783-793.	0.3	4

#	Article	IF	CITATIONS
109	Thermo-elastic behavior and P/T phase stability of TIAlSiO4 (ABW). Microporous and Mesoporous Materials, 2014, 197, 262-267.	2.2	3
110	Plumbopharmacosiderite, Pb <sub>0.5</sub> Fe <sup>3+</sup> <sub>4</sub> (AsO <sub>4</sub> ) <sub>3</sub> (OH) <sub>4</sub> ·5H <s A New Mineral Species From the Monte FalÃ<sup>2</sup> Pb-Zn Mine Near the Village of Coiromonte In the Armeno Municipality, Novara Province, Italy. Canadian Mineralogist, 2018, 56, 143-150.</s 	ub>2 <td>o&gt;<u>0</u>,</td>	o> <u>0</u> ,
111	On the Swelling Behaviour of Weak Rocks Due to Gypsum Crystallization. Procedia Engineering, 2016, 158, 128-133.	1.2	1
112	Thermo-elastic behaviour of Be2BO3OH (hambergite) up to 7ÂGPa and 1,100ÂK. Physics and Chemistry of Minerals, 2013, 40, 401-409.	0.3	0
113	High-pressure and high-temperature structure and equation of state of Na <sub>3</sub> Ca <sub>2</sub> La(CO <sul burbankite. European Journal of Mineralogy, 2022, 34, 351-358.</sul 	o>	3